DINAME 2023 - Proceedings of the XIX International Symposium on Dynamic Problems of Mechanics,
A.S. De Paula, A.T. Fabro and M.R. Machado (Editors), ABCM.
Pirenópolis, Go, Brazil, February 26th to March 3rd, 2023

Nonlinear dynamics of an origami-stent

Guilherme V. Rodrigues [1] and Marcelo A. Savi [2]

[1] Universidade Federal do Rio de Janeiro, guilherme_@live.co.uk

[2] Universidade Federal do Rio de Janeiro, savi@mecanica.coppe.ufrj.br

Abstract: Origami has inspired innovative engineering designs. A cylindrical origami-stent is analyzed in this work considering shape memory alloy actuators for fold/unfold the structure. Nonlinear dynamics is of concern considering two reduced order models represented by single-row and 2-row. Numerical simulations are carried out evaluating the influence of external forces. Complex responses are achieved including chaos.

Keywords: origami, smart actuation, nonlinear dynamics

INTRODUCTION

Origami-inspired devices refer to the application of the art of origami, the ancient technique of folding paper to create three dimensional structures from two dimensional sources. Origami-inspired systems and structures have a growing importance in several areas of human knowledge, being associated with innovative designs (Fonseca *et al.*, 2022). Origami-based designs are essentially based on geometrical properties, being implemented from nano to giga scale. Therefore, it has found applications in several areas, as biomedical engineering, architecture, and metamaterials.

On the last years, there is an increase in articles on origami-based designs that cover relevant aspects as fabrication, thickness accommodation and actuation (Meloni *et al*., 2021). Smart materials capable of convert various forms of energy into mechanical work have been applied to accomplish the folding behavior, creating self-folding origami (Hernandez *et al*., 2014). The capability of perform folding/unfolding operations without being kinematically manipulated by external forces is advantageous for several designs as small-scale devices and space systems applications.

Most origami investigations have focused on their geometry, kinematics, and quasi-static mechanics. Considering the high nonlinearity of origami geometry, their dynamical responses are rich and complex. Besides, origami-inspired devices are commonly embedded in mechanical systems that are externally excited, as for example in robotics vehicles, impact and vibration isolation structures and energy harvesting devices.

This paper deals with the nonlinear dynamics of the origami-stent, a cylindrical self-folding origami-inspired structure firstly designed to be employed as a tubular medical device used to protect weakened arterial walls in the human body (Kuribayashi *et al*., 2006). The origami-stent is actuated by torsional shape memory alloy (SMA) springs. A single row and a two-row reduced order model are of concern, and their differences are compared under dynamical excitations.

MATHEMATICAL MODEL

The origami-stent is a built from the tessellation of the waterbomb pattern. The waterbomb pattern consists of six creases, two mountains and four valley creases, around a central vertex (Fig. 1). The sheet with the waterbomb pattern is closed in a cylindrical shape to create the origami-stent.

Thus, the kinematic of the origami-stent is related to the kinematic of the waterbomb pattern. It is defined as unit cell each portion of the waterbomb pattern tessellated in origami. Considering the rigid origami theory, the unit cell can be described with three degrees of freedom (3-DoF) (Fonseca *et al*., 2021) and, naturally, the tessellated structure has multiple degrees of freedom. However, symmetry hypotheses can be stablished in order to define a proper number of degrees of freedom (Chen *et al*., 2016). Rodrigues *et al*. (2021) show that the unit cell can be described as 2-DoF system if a plane of symmetry is considered. Besides, the origami-stent is a 2-DoF as well when circumferential symmetry is taken into account (Imada *et al*., 2022).

The unit cell presented in Fig. 2 is described by the angles θ_R, θ_L, $2\varphi = \varphi_R + \varphi_L$ with the *xz*-plane as the plane of symmetry. Since no deformations are allowed on a rigid origami, the constraint $\overline{B_1 B'_1} = 2L$ leads to the following equation:

$$\tan^2(\alpha_0)\,[\cos\theta_L \cos\theta_R\,(\cos(2\varphi)) - \sin\theta_L \sin\theta_R + 1] + \tan(\alpha_0)\,[\sin(2\varphi)\,(\cos\theta_L + \cos\theta_R)] - \cos(2\varphi) = 1 \quad (1)$$

The unit cells are circumferentially distributed in origami-stent (Fig. 2), being characterized by a radius defined by Eq. (2), where n is the number of unit cells.

$$\rho = \frac{\bar{\rho}}{L} = \frac{1}{\tan\left(\frac{\pi}{n}\right)}\tan(\alpha_0)\sin(\theta_R) - \cos(\varphi_R) + \tan(\alpha_0)\sin(\varphi_R)\cos(\theta_R) \tag{2}$$

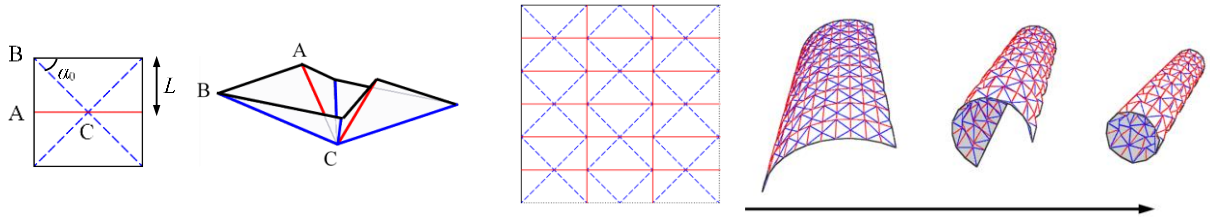

Figure 1 – The waterbomb pattern consists of two mountain creases and four valley creases. A sheet with a tessellation of the waterbomb pattern is closed in a cylindrical shape to create the origami-stent.

Origami-stent is made of several rows shifted each other of half- unit cell. The mutual vertices in adjacent rows allows one to find a relation between adjacent rows. For instance, considering the index j to indicate the row, Fig. 2 shows that vertex $A_{j=1}$ is equivalent to $B'_{2\,j=2}$ and $B_{1\,j=1}$ is equivalent to $A'_{j=2}$. Therefore, the following equations are found:

$$\theta_{L\,j+1} = \sin^{-1}\left(\frac{1}{\tan(\alpha_0)}\sin\left(\frac{\pi}{n}\right)\left(\rho_j + \cos\left(\varphi_{R\,j}\right)\right)\right) \tag{3}$$

$$\varphi_{L\,j+1} = \sin^{-1}\left(\frac{\sin\left(\theta_{R\,j}\right) - \sin\left(\theta_{L\,j+1}\right)\cos\left(\frac{\pi}{n}\right)}{\cos\left(\theta_{L\,j+1}\right)\sin\left(\frac{\pi}{n}\right)}\right) \tag{4}$$

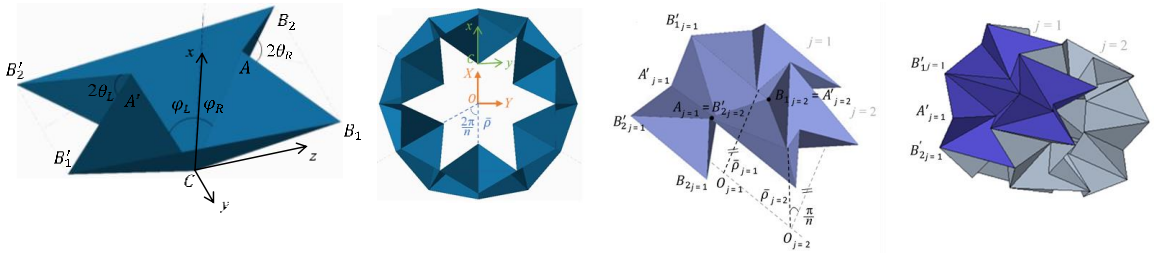

Figure 2 – Origami-stent is represented by n unit cells circumferentially distributed in several rows.

The geometric relations established allow to describe the origami-stent with several rows as a simple 2-DoF system. Rodrigues *et al*. (2021) show that one can go further on symmetry hypotheses by halving the origami-stent, leading to a 1-DoF system. In this work, only a single row and a 2-rows origami-stent are on focus. For the sake of simplicity, a 1-DoF system is considered. Aiming so, it is considered $\theta_R = \theta_L$ for the single row case and $\theta_{R(j=1)} = \theta_{L(j=2)}$ for the 2-rows case. In other words, the unit cells of a single row origami-stent behavior symmetrically on *xz*-plane and on *xy*-plane while the unit cells of the 2-rows origami-stent behavior symmetrically on *xz*-plane and the rows have mirrored behaviors.

Once the kinematics is well exploited, the dynamics of the origami-stent is described. It is considered the movement of the facets of the unit cells. Each triangular facet rotates with an angular velocity $\bar{\boldsymbol{\omega}}$ presenting inertia $\boldsymbol{I}$ (Rodrigues *et al*., 2017). Thus, the kinetic energy E is described as:

$$E = \left(\bar{\boldsymbol{\omega}}_{AB_1C}\right)^{\boldsymbol{T}} \boldsymbol{I}_{AB_1C}\bar{\boldsymbol{\omega}}_{AB_1C} + \left(\bar{\boldsymbol{\omega}}_{B_1B'_1C}\right)^{\boldsymbol{T}} \boldsymbol{I}_{B_1B'_1C}\bar{\boldsymbol{\omega}}_{B_1B'_1C} + \left(\bar{\boldsymbol{\omega}}_{A'B'_1C}\right)^{\boldsymbol{T}} \boldsymbol{I}_{A'B'_1C}\bar{\boldsymbol{\omega}}_{A'B'_1C} \tag{5}$$

Actuation on origami-stent is provided by a torsional SMA springs with length L_S and radius r_S (Koh *et al*., 2014). A pair of springs is placed along creases AC and A'C of each unit cell. Their thermomechanical behavior is described by a polynomial constitutive model (Falk, 1980) that relates moment-angle-temperature:

$$M_{SMA}(\theta) = \frac{\pi {r_s}^3}{2}\left(a_1(T - T_M)\left(2\frac{r_s}{L_s}\theta - 2\frac{r_s}{L_s}\theta_I\right) - a_2\left(2\frac{r_s}{L_s}\theta - 2\frac{r_s}{L_s}\theta_I\right)^3 + a_3\left(2\frac{r_s}{L_s}\theta - 2\frac{r_s}{L_s}\theta_I\right)^5\right) \tag{6}$$

where a_1, a_2 and a_3 are material parameters, T_M is the temperature below which the martensitic phase is stable and θ_I is the angle where the spring is free of stress.

Variable θ_R is assumed to be the generalized coordinate and an external generalized force F_{ext} is applied at the central vertex C in the radial direction, $\bar{\rho}$-direction. Besides, a linear viscous dissipation with coefficient ζ is considered representing all dissipation processes, including hysteresis. Therefore, Lagrange's equation furnishes the equation of motion:

$$\frac{\partial}{\partial t}\left(\frac{\partial E}{\partial \dot{\theta}_R}\right) - \left(\frac{\partial E}{\partial \theta_R}\right) = -\zeta\dot{\theta}_R - M_{SMA}(\theta_R) - M_{SMA}(\theta_L)\,\partial\theta_L/\partial\theta_R + F_{ext}\,\partial\bar{\rho}/\partial\theta \tag{7}$$

NUMERICAL SIMULATIONS

Numerical simulations are performed by considering the fourth-order Runge-Kutta method employed to a nondimensional version of the equation of motion and parameters presented in Table 1.

Table 1 – Set of parameters assumed in numerical simulations.

Waterbomb length L	Unit cell mass	Damping coefficient ζ
6.6 mm	0.30 g	0.3 N s/m
Spring length L_s	Spring radius r_s	Temperature T_M
2.2 mm	0.08 mm	287.15 K
SMA parameter a_1	SMA parameter a_2	SMA parameter a_3
1.0 MPa/K	1.4×10^4 MPa	2.2×10^4 MPa

A comparison for the two reduced-order models of the origami-stent with a single row and with 2 rows are settled hereafter considering different external loads. A bifurcation diagram is presented in Fig. 3 for μ = 0.06 and varying the frequency ω from 0.05 to 0.20. For a single row, chaotic-like responses are found between ω = 0.09 and 0.125, otherwise a 1-period is observed. Considering 2 rows, chaotic-like behavior is found up to ω = 0.16, then period-1 and period-2 responses are found with a bifurcation at ω = 0.17. In both cases, periodic responses can be found inside the chaotic-like window as, for example, the period-2 responses between ω = 0.08 and 0.09 for 2 rows.

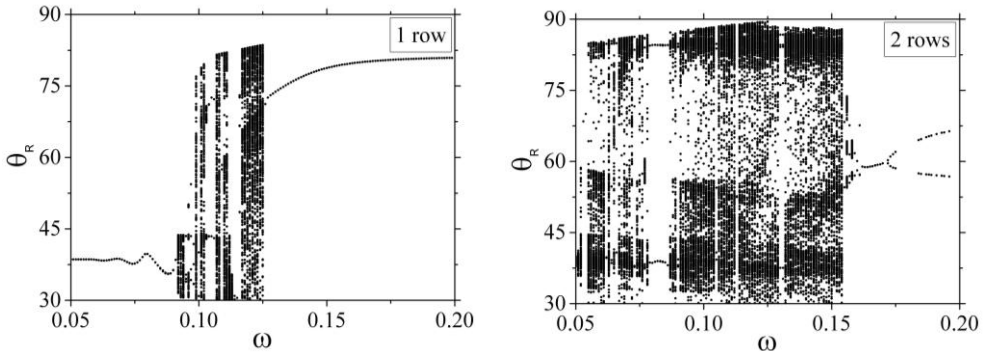

Figure 3 – Bifurcation diagrams varying frequency ω (μ = 0.06).

Fig. 4 presents results for two different cases: a chaotic response at ω = 0.12 and a period-1 response at ω = 0.17. Time histories are presented in the top of the figure and phase spaces with Poincaré sections are presented at the bottom. The Poincaré section allows to identify the strange attractor of each system.

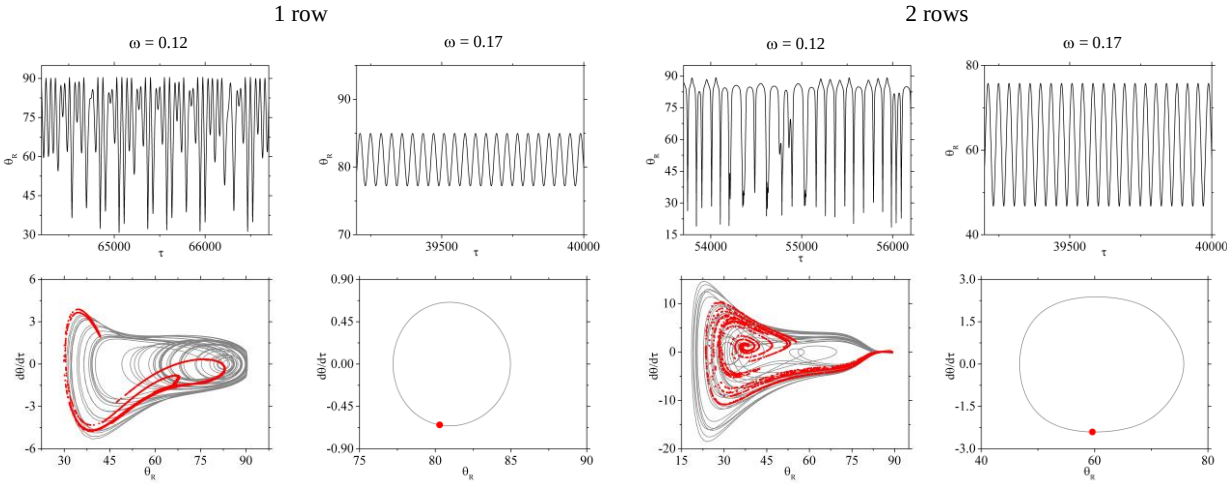

Figure 4 – Chaotic and periodic responses (μ = 0.06). Poincaré sections presented as red dots.

Let us now explore the dynamical response of the system at $\omega = 0.12$. Fig. 5 presents the bifurcation diagrams by varying the force amplitude μ from 0.05 to 0.07. Considering a single row, the chaotic response at $\mu = 0.06$ (Fig. 4) becomes periodic at lower force amplitudes, especially for $\mu < 0.055$. For 2 rows, the chaotic response at $\mu = 0.06$ (Fig. 4) becomes periodic both at lower and higher force amplitudes. 1-period responses are found for $\mu < 0.0515$, 3-period responses are found for $\mu > 0.0642$ and between these values the system behavior is mainly chaotic-like.

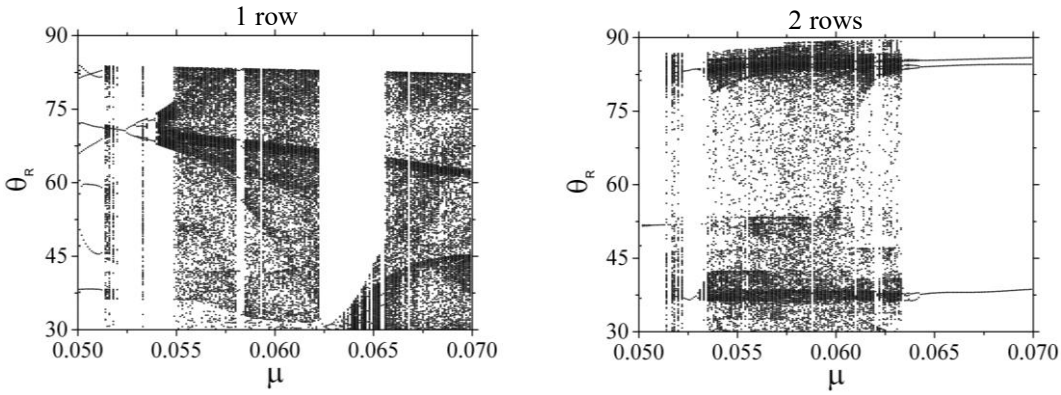

Figure 5 – Bifurcation diagrams varying amplitude μ ($\omega = 0.12$).

REFERENCES

Meloni, M., Cai, J., Zhang, Q., Sang‐Hoon Lee, D., Li, M., Ma, R., Parashkevov, T. E. & Feng, J. (2021). Engineering Origami: A comprehensive review of recent applications, design methods, and tools. Advanced Science, 2000636.

Hernandez, E. A., Hartl, D. J., Malak Jr, R. J., & Lagoudas, D. C. (2014). Origami-inspired active structures: a synthesis and review. Smart Materials and Structures, 23(9), 094001.

Kuribayashi, K., Tsuchiya, K., You, Z., Tomus, D., Umemoto, M., Ito, T., & Sasaki, M. (2006). Self-deployable origami stent grafts as a biomedical application of Ni-rich TiNi shape memory alloy foil. Materials Science and Engineering: A, 419(1-2), 131-137.

Fonseca, L. M., & Savi, M. A. (2021). On the symmetries of the origami waterbomb pattern: kinematics and mechanical investigations. Meccanica, 56(10), 2575-2598.

Fonseca, L. M., Rodrigues, G. V., & Savi, M. A. (2022). An overview of the mechanical description of origami-inspired systems and structures. International Journal of Mechanical Sciences, 223, 107316.

Chen Y., Feng H., Ma J., Peng R., & You Z. (2016). Symmetric waterbomb origami. In Proceedings of the Royal Society A: Mathematical, Physical and Engineering Sci, 472 (2190), Art. ID 20150846.

Rodrigues, G. V., & Savi, M. A. (2021). Reduced-order model description of origami stent built with waterbomb pattern. International Journal of Applied Mechanics, 13(02), 2150016.

Imada, R., & Tachi, T. (2022). Geometry and Kinematics of Cylindrical Waterbomb Tessellation. Journal of Mechanisms and Robotics, 14(4), 041009.

Rodrigues, G. V., Fonseca, L. M., Savi, M. A., & Paiva, A. (2017). Nonlinear dynamics of an adaptive origami-stent system. International Journal of Mechanical Sciences, 133, 303-318.

Falk, F. (1980). Model free energy, mechanics, and thermodynamics of shape memory alloys. Acta Metallurgica, 28(12), 1773-1780.

Koh, J., Kim, S., & Cho, K. (2014). Self-Folding Origami Using Torsion Shape Memory Alloy Wire Actuators. In Proceedings of the ASME 2014 International Design Engineering Technical Conferences and Computers and Information in Engineering Conference, 5B: 38th Mechanisms and Robotics Conference, V05BT08A043.